Search for radio echoes from EAS with the MU radar, Shigaraki, Japan

Toshio Terasawa*, **Takuji Nakamura**†, **Hiroyuki Sagawa**‡, **Hideaki Miyamoto**‡, **Hideto Yoshida**‡ **and Masaki Fukushima**‡

**Tokyo Institute of Technology*
†*National Institute of Polar Research*
‡*University of Tokyo*

Abstract. We have made a trial search for radar echoes from extended air showers of ultra high energy cosmic rays. We present a summary of basic system description/methodology and preliminary results.

Keywords: UHECR, EAS, radar

I. Introduction

Wide attention has been attracted to the detection of ultra high energy cosmic rays (UHECR) with radio techniques, either passive [1][2] and active [3][4][5][6], towards future large-scale UHECR observatory on the ground. This paper is a progress report on our trial of the active method, namely, the trial toward the detection of radar echoes from extensive air showers (EAS) of UHECRs (EAS echoes, hereafter).

Figure 1 shows the geometry under consideration. At the head of an EAS, there are relativistic shower particles forming a thin disk. Behind the disk there are products of ionization by these relativistic particles, namely thermal~suprathermal free electrons along the shower axis. What we are trying to detect is a specularly reflected echo by these free electrons.
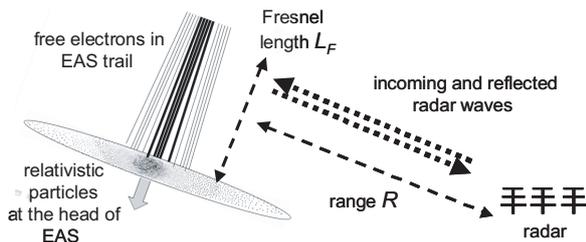

Fig. 1: The geometry for a specularly reflected radar echo by free electrons produced in the trail region of an EAS.

Since we consider the coherent reflection process, the effective length of the reflection is given by the Fresnel length,

$$L_F = \sqrt{2R\lambda}$$

where R is the range distance between the radar and the EAS, and λ the wavelength of the radar wave. With $R \sim$10-30 km and $\lambda \sim$several m (for the VHF band radar), we have $L_F =$300-600m. The duration of an EAS echo is expected to be the order of $L_F/c + \tau_e$ (c: the speed of light=2.99792458$\times 10^8$m sec^{-1}), where the first term (1-2μsec) is the travel time of relativistic particles for the distance L_F, and the second the life time of the free electrons. In his pioneering work [3], Gorham estimated τ_e to be in the range of 20 μsec $\sim$ 20msec. However, this estimation seems too optimistic, and τ_e is more likely to be several μsec or shorter [7].

In what follows, we show the radar-system setup and preliminary results of the trial observation of EAS echoes. For a conclusive identification of EAS echoes, of course, we need to take a coincidence between the radio and particle observations. Such attempts are to be planned once the physical parameters of likely EAS echo candidates (echo time profile, duration, intensity, etc.) are obtained.

Fig. 2: The MU radar in Shigaraki, Japan (136°E06'32", 34°N51'08").

II. MU radar: System description and echo-search methodology

We utilize the MU radar in Shigaraki, Japan (Figure 2), a high-power (peak:1MW, average:50kW) mono-static pulse Doppler radar with the central frequency f=46.5MHz (the wavelength $\lambda = c/f = 6.447$m), which is operated by the Research Institute for Sustainable Humanosphere (RISH) of Kyoto University. The MU radar consists of 475 sets of 3-element crossed-Yagi antennas, which are placed regularly with the span of 4.5m (plus symbols in Figure 3) to fill the circular area (8330m^2) of a diameter $D = 103$m. The phase at each of 475 antennas is changed by an 8-bit phase shifter (1.4° resolution) for both transmission and reception

independently, which enables to form different beam patterns for transmission and reception.

[Transmission beam pattern] While the highest angular concentration obtainable in the MU radar is $\lambda/D \sim 3.6°$, we have widened the transmission beam pattern as shown in Figure 4 [8] in order to increase the detection possibility of EAS echoes, whose incident directions are expected to be isotropic. For the trial observations made in 2008, the sky area of zenith angle $\theta \leq 50°$ was illuminated by the transmission beam with the relative intensity $-15 \sim 0$dB. There are $\sim$-20dB side lobes near the horizontal direction ($\theta \sim 90°$), which cause ground clutter echoes for the range $R < \sim 19$km.

[Reception beam pattern] At reception, the 475 antennas are divided into 25 groups. An independent digital receiving system is connected to each of the 25 groups so as to configure a 25 channel spatial-domain interferometer. For the antenna selection from each of these groups, we have two options. One is a wide beam option where we choose one antenna from each of 25 groups (shown by circles in Figure 3) so as to maximally widen the sky coverage of the interferometer at the cost of sensitivity. The other is a narrow beam option where we connect all 19 antennas in each group with the corresponding digital receiver system so as to maximize the sensitivity with a narrow sky coverage. In this paper we report the results with the former option.
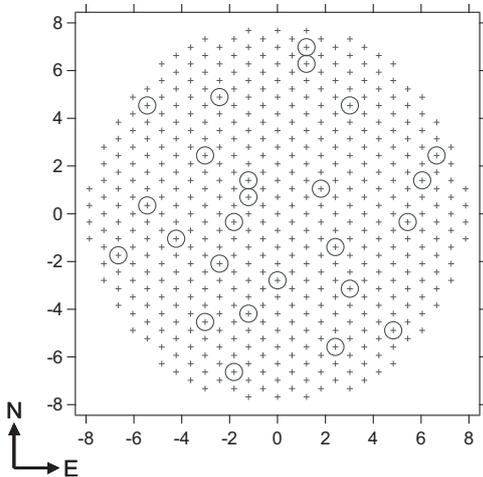
Fig. 3: The spatial antenna configuration of the MU radar. Horizontal and vertical axes respectively point toward the east and north directions, where the length scales are in the wavelength unit.

[Inter-pulse period and pulse length] The MU radar is a pulse radar, so that transmission and reception sequences are switched alternatively. The inter-pulse period (IPP) is set to be 4msec so as to avoid effects of range-aliasing meteor echoes from the altitude 80-120km. Meteor echoes of the range R> 600km, which cause range aliasing even for the choice of IPP=4msec, were rare but observed in a few occasion during the test operation of the MU radar prior to the EAS echo search.
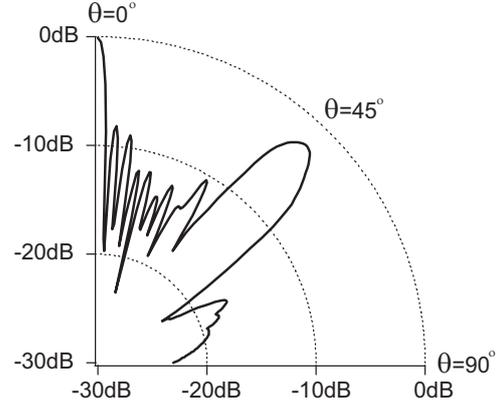
Fig. 4: The transmission beam pattern of the MU radar in the zenith-horizontal cross section,

Care will be taken to eliminate such long-range meteor echoes.

The pulse length Δt is set at 64μsec. Since the duration of EAS echoes is expected to be shorter than Δt, their range determination has uncertainty of $\Delta R = \pm c\Delta t/4 = \pm 4.8$km. This uncertainty could be reduced if, for example, the CW/FM (continuous-wave and frequency-modulated) radar technique is introduced. However, we defer it as a possible future extension.

[Signal reception] At the signal reception the MU system allows us to select the sampling interval $\delta t \geq 0.5\mu$sec. δt as short as possible is desirable to resolve the time profile of EAS echoes. On the other hand, however, the noise level as well as the demand for data buffer storage is raised inversely proportional to δt. We have chosen then a moderate value of 2μsec.

We process the complex voltages $I_\ell + iQ_\ell$ with $\ell = 1, ...25$ of the sampled data following the usual aperture synthesis technique in radio astronomy (e.g.,[9]). First we make cross products,

$$C_{\ell,m} \equiv (I_\ell + iQ_\ell)(I_m - iQ_m) \qquad (1)$$

for $\ell = 1, ...25$ and $m = 1, ...25$. The brightness temperature $T_b(\vec{k})$ for the wavenumber vector $\vec{k} = (k_x, k_y, k_z)$ is obtained via discrete Fourier transformation,

$$T_b(\vec{k}) = \alpha \sum_{\ell,m} C_{\ell,m} \exp\left\{ i\vec{k} \cdot (\vec{r}_\ell - \vec{r}_m) \right\} \qquad (2)$$

where α is a conversion factor from the signal strength to the brightness temperature, and $\vec{r}_\ell$ and $\vec{r}_m$ are the positions of the ℓ-th and m-th antennas on the ground, $(x_\ell, y_\ell, 0)$ and $(x_m, y_m, 0)$, respectively.

[EAS echo search] To search EAS echo candidates, we select wavevectors $\vec{k}_\#$ with $\# = 1, ...1423$ covering the zenith angle $0 \leq \theta_\# \leq 50°$ and the azimuthal angle $0 \leq \varphi_\# < 360°$. (Following the geophysical convention, we take $\varphi = 0°$ and $90°$ for the north and the east directions, respectively.) Here $\theta_\#$ and $\varphi_\#$ are for the

looking direction, from which we obtain

$$k_{\#,x} = -\frac{2\pi}{\lambda} \sin(\theta_\#) \sin(\varphi_\#),$$

$$k_{\#,y} = -\frac{2\pi}{\lambda} \sin(\theta_\#) \cos(\varphi_\#).$$

The 1423 sets of $T_{\rm b}(\vec{k}_\#)$ (we call it 'a $T_{\rm b}$ sky map', hereafter) are calculated with the time interval of $\delta t = 2\mu$sec (or the range interval $\delta R = c\delta t/2 = 300$m) for $R_{\min} = 18.9$km $\leq R \leq R_{\max} = 40.5$km. The data for $R < 18.9$km are not included to avoid the ground clutter echoes. Now the following procedure is taken:

1) Search a unique brightest spot on each of $T_{\rm b}$ sky maps with signal to noise ratio (SNR) above 10dB.
2) Choose the spots from those identified in 1) that appear also on the $T_{\rm b}$ sky maps produced from the subgroups of antennas, such as the east/west or north/south subgroups of antennas.
3) Select the spots from those chosen in 2) whose life times are longer than 2μsec but less than one IPP (4msec). Namely, the spot should appear at least two neighboring maps with the interval $\delta t = 2\mu$sec, but not on the maps for the previous/next radar pulses. The former criteria is to identify the events of high statistical significance, while the latter rejection criteria is to eliminate possible contamination of long-range meteor echoes.

III. TRIAL SEARCH FOR EAS ECHOES

We made trial observations after September 2008. During the time of the high human activity, it is found that strong echoes from aircraft penetrating through the antenna sides lobe were often overwhelming, and that meaningful EAS echo search becomes difficult, if not impossible. The best interval for the EAS echo search is between 01:00 LT and 05:00 LT, when the human activity is minimized. We made 4 night observations including this best LT interval and accumulated data for 14 hours. Since the discrete Fourier transformation in (2) is time consuming, we could so far process 2 hours of the data. Applying the procedure described in the previous section, we have found an EAS echo candidate as shown in Figure 5a, where the $T_{\rm b}$ sky map for the range $R = 24 \pm 4.8$km at 11:31:53.624 UT (02:31:53.624 LT) on 3 December 2009 is drawn. This EAS echo candidate (indicated by an arrow) was found at the direction of the zenith angle $\theta = 12°$ and the azimuthal angle $\varphi = 185°$. To see the effect of the antenna side lobe, a simulated sky map for the point source at $(\theta, \varphi) = (12°, 185°)$ is drawn in Figure 5b, where the peaks fainter than the main peak represent this effect. Some of the faint peaks in Figure 5a are thus explicable in terms of the side lobe effect caused by the main peak signal.

The time variation of $T_{\rm b}$ is shown in Figure 5c, where the horizontal axis shows the time (μs) elapsed from the peak. A line with solid squares shows $T_{\rm b}$ at the peak
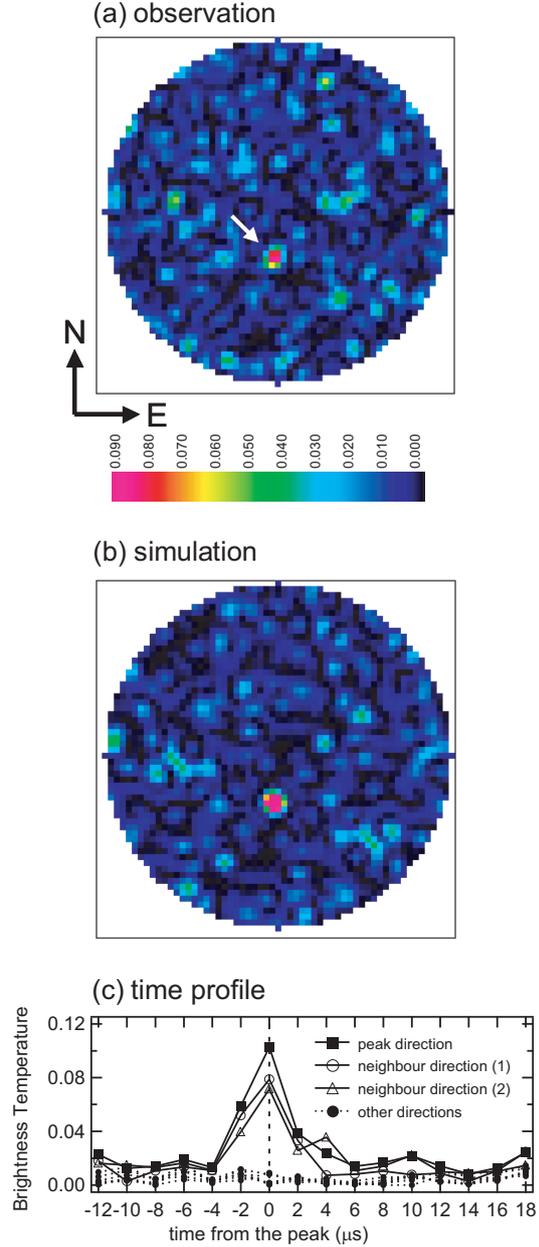

Fig. 5: (a) Observed $T_{\rm b}$ sky map within the sky area of the zenith angle $\theta \leq 50°$, where $T_{\rm b}$ is shown in an arbitrary unit. On the map the center corresponds to the zenith, and the distance from the zenith is taken proportional to $\sin\theta$. (b) The same as (a) but for a simulated $T_{\rm b}$ sky map. (c) The time variation of $T_{\rm b}$.

direction $(\theta_p, \varphi_p) = (12°, 185°)$. We see that the duration of the echo was 4-6μs, which is close to the duration expected for EAS echoes (see the introduction section). Other lines are for directions $\pm 6°$ away from the peak either in the zenith or azimuthal directions, in which $(12°, 179°)$ and $(12°, 191°)$ corresponding to the east and west directions neighboring to the peak direction are drawn with open circles and triangles, respectively. That the echo intensities in the peak and these two directions are higher than the other directions means that the echo

image was elongated in the east-west direction.

IV. SUMMARY AND COMMENT

We have presented the method and preliminary results of our trial search for EAS echoes using the MU high-power mono-static radar. It is noted that our EAS echo candidate shown in Figure 5 has some resemblance to what Wahl et al. [6] found in their Jicamarca radar experiment. However, while Jicamarca echoes were limited to the zenith angle less than $0.5°$ and the range $R > 25$km, our echo candidate had the zenith angle of $12°$ and the altitude less than 25km.

After obtained one EAS echo candidate, we have re-searched similar echoes within the dataset so far processed, and found several tens of bright spots in the T_b sky maps which satisfy the criteria 1) and 2) but not 3) since they appeared in only one 2μsec interval.

Our next plan is to shorten the sampling interval δt toward the hardware limit of the MU radar system, 0.5μsec. The shortening of δt alone does not suffice since it raises the noise level at the same time. We will combine the improvement of the antenna gain by reshaping the transmission and reception beam patterns with the optimization of δt.

REFERENCES

[1] H. Falcke *et al.* : Nature, 435, 313, 2005.
[2] P. W. Gorham *et al.* : arXiv:0705.2589v1 [astro-ph], 2007.
[3] P. W. Gorham: Astroparticle Phys., 15, 177, 2001.
[4] A. Iyono *et al.* : Proc. 28th Int. Cosmic Ray Conf., Tsukuba, 2003.
[5] D. O. Damazio: Nucl. Phys. B (Proc Suppl) 134, 217, 2004.
[6] D. Wahl, J. Chau, and J. Bellido: Proc. 30th Int. Cosmic Ray Conf., Merida, 2007.
[7] R. J. Vidmar: IEEE Trans. on Plasma Science, 18, 733, 1990.
[8] T. Nakamura: Radio Science, 26, 857, 1991.
[9] A. Thompson *et al.* , ed.; Interferometry and Synthesis in Radio Astronomy, Wiley-VCH, 2004.